Progress in Nuclear Energy 131 (2021) 103580

Contents lists available at ScienceDirect

Progress in Nuclear Energy

journal homepage: http://www.elsevier.com/locate/pnucene

A semi-supervised method for the characterization of degradation of nuclear power plants steam generators

Luca Pinciroli [a], Piero Baraldi [a,*], Ahmed Shokry [a,b], Enrico Zio [a,c,d], Redouane Seraoui [e], Carole Mai [e]

[a] Energy Department, Politecnico di Milano, Via Lambruschini 4, 20156, Milan, Italy
[b] Center for Applied Mathematics, Ecole Polytechnique, Route de Saclay, 91120, Palaiseau, France
[c] MINES ParisTech, PSL Research University, CRC, Sophia Antipolis, France
[d] Eminent Scholar, Department of Nuclear Engineering, College of Engineering, Kyung Hee University, Republic of Korea
[e] Électricité de France R&D, 6 Quai Watier, Chatou, France

ARTICLE INFO

Keywords:
Condition-based maintenance
Degradation assessment
Semi-supervised
Feature selection
Nuclear power plant
Steam generator

ABSTRACT

The digitalization of nuclear power plants, with the rapid growth of information technology, opens the door to the development of new methods of condition-based maintenance. In this work, a semi-supervised method for characterizing the level of degradation of nuclear power plant components using measurements collected during plant operational transients is proposed. It is based on the fusion of selected features extracted from the monitored signals. Feature selection is formulated as a multi-objective optimization problem. The objectives are the maximization of the feature monotonicity and trendability, and the maximization of a novel measure of correlation between the feature values and the results of non-destructive tests performed to assess the component degradation. The features of the Pareto optimal set are normalized and the component degradation level is defined as the median of the obtained values. The developed method is applied to real data collected from steam generators of pressurized water reactors. It is shown able to identify degradation level with errors comparable to those obtained by ad-hoc non-destructive tests.

1. Introduction

Since early 1990s the nuclear industry has increased its interest in fault detection, diagnostics and prognostics with the objectives of improving the overall safety and efficiency of Nuclear Power Plants (NPPs) operation (Tambouratzis et al., 2019). In particular, the data that are collected from the plants and the availability of machine learning methods make possible to implement Condition-Based Maintenance (CBM) practices (Ayo-Imoru and Cilliers, 2018). CBM can contribue to: *i*) plant safety by reducing the probability of abnormal conditions caused by component failures, *ii*) reducing the number of unplanned corrective maintenance interventions, that are typically very expensive and time consuming, *iii*) increasing the overall plant availability, with tangible benefits in terms of production profit, *iv*) shortening outages (Tsang, 1995; Shin and Jun 2015; Ayo-Imoru and Cilliers, 2018; Uchida et al., 2019).

In (IAEA, 2008) a detailed description of a variety of established techniques for online condition monitoring of NPPs equipment and systems is presented. In (Coble et al., 2012, 2015) the current state of monitoring, prognostics, and health management for different NPPs components is reviewed. In (Tambouratzis et al., 2019) a review of the computational intelligence methodologies developed from 1990 to 2015 for NPPs control, fault detection and diagnostics is provided. In (Saeed et al., 2020) a novel fault diagnostic method based on principal component analysis, long short-term memory and convolutional neural network is proposed. In (Wang et al., 2019) a hybrid fault diagnosis methodology based on support vector machine and particle swarm optimization is proposed and applied to NPPs.

According to the International Energy Agency (IEA), the saving from the digitalization of the overall power sector is going to be in the order of $80 billion per year over the period 2016–2040, or about 5% of the total annual power generation cost (IEA, 2017). Specifically to nuclear industry, information technology and digitalization can contribute to address major challenges, such as improving operational efficiency, life extension and renewal with new reactor designs (Huffeteau, 2016; Faudon, 2018).

* Corresponding author.
E-mail address: piero.baraldi@polimi.it (P. Baraldi).

https://doi.org/10.1016/j.pnucene.2020.103580
Received 16 January 2020; Received in revised form 27 October 2020; Accepted 19 November 2020
Available online 4 December 2020

This work falls within the ongoing digital transition of NPPs and the potential transformation of maintenance.

The key quantity of interest in CBM is the degradation level of the nuclear components, whose measure, depending on the component and its degradation mechanisms, can be directly available, e.g., the length of a crack, the thickness of a deposit, or must be inferred from monitoring signals, e.g., vibration signals for bearing wear (Shen et al., 2012), capacity for battery degradation (Ansean et al., 2017), depolarization current for the degradation of polymeric insulation of power cables (Abou-Dakka et al., 2011). Since in practice it is difficult to identify a single, directly measurable physical quantity correlated to the component degradation level, in this work we develop a method to infer the component degradation level from monitored signals.

The problem of extracting features correlated to the component degradation level from monitored signals has been already addressed for various components in different industrial applications. Considering, for example, rolling mechanical components such as bearings, vibration signals are typically used for inferring their degradation level. For example, in (Qiu et al., 2003) a combination of wavelet transform and self-organizing map is used to derive a degradation indicator; in (Ben Ali et al., 2015) an artificial neural network, which receives in input time-domain features and features obtained by applying the Empirical Mode Decomposition (EMD) transform to the energy entropy, is used to identify component degradation. The main constraint of these methods is that they require prior knowledge on the component degradation level. In (Gomes et al., 2016) several monitored signals are combined into a unique degradation indicator for electro-mechanical actuators and auxiliary power units through the use of nonparametric density estimation techniques and the Runger's U^2 method. This method requires an adequate estimation of the underlying probability distributions through a careful acquisition of data, which is not always possible in practice. In (Kumar et al., 2012), a degradation indicator based on the Mahalanobis distance is proposed and applied to electronic products. Since this method is based on the assumption that a subset of the monitored signals correlated to the component degradation has been a priori identified, its application is limited to those systems for which signals related to degradation are known. In (Coble and Hines, 2009) a set of metrics evaluating the goodness of a parameter as degradation indicator has been proposed and the metrics are used within a Genetic Algorithm (GA) optimization routine to identify an optimal degradation indicator for turbofan engines. In (Baraldi et al., 2018), a method based on the combined use of EMD, Auto-Associative Kernel Regression and a multi-objective Binary Differential Evolution (BDE) algorithm is proposed for selecting the subset of optimal features for the definition of a degradation indicator for turbofan engines.

In this work, we propose a novel method for the identification of the degradation level of industrial components on the basis of the evolution of monitored signals during plant operational transients.

The proposed methodology is based on the three steps of feature extraction, feature evaluation and feature selection. In the first step, possible informative features (such as mean, variance, wavelet coefficients, wavelet energy, etc.) are extracted from the monitored signals collected during operational transients. In the second stage, the goodness of the extracted features are systematically evaluated with respect to specific metrics that represent generic, preferable properties of degradation indicators (Coble and Hines, 2009; Coble, 2010; He et al., 2015), namely monotonicity and trendability, and a novel metric of correlation between the feature values and the results of the Non-Destructive Tests (NDTs), which is termed "correlability". Then, the problem of selecting the features for the construction of the degradation indicator is framed as a multi-objective optimization problem and the features of the Pareto optimal set are aggregated taking the median as degradation indicator.

The proposed method is applied to the identification of the degradation level of Steam Generators (SGs) in Nuclear Power Plants. This is an important task, given that SGs are among the most critical components in NPPs, since the power production depends on their functioning. The performance of the proposed method is shown using real data collected during 25 years of operation of two fleets of SGs in NPPs operated by Électricité de France (EDF).

The main contributions of the work are:

1) The use of both the Mann-Kendall test and monotonicity index defined in (Coble and Hines, 2009) for the evaluation of the monotonicity of the extracted features;
2) The definition of the correlability index, based on Spearman correlation coefficient, for the evaluation of the correlation between the extracted feature and the results of the NDTs;
3) The combined use of the large amount of (unsupervised) signal monitoring data, as in (Coble and Hines, 2009) and in (Baraldi et al., 2018), and of the small amount of very informative (supervised) data collected during NDTs for the definition of the degradation indicator.
4) the use of plant data collected during operational transients for degradation assessment. According to (Sharp, 2012; Girard, 2014), they are more informative about the component degradation than data collected during steady state operation;
5) The application of the developed method to NPP SGs. At the best of our knowledge, no degradation indicator based on measurements is currently used in the nuclear industry.

The rest of the paper is organized as follows. Section 2 introduces the problem of degradation of SG in NPPs. Section 3 formulates the problem statement. Section 4 presents the method developed for the definition of the degradation indicator. Section 5 describes the validation procedure. Section 6 presents the SG case study and the real datasets. Section 7 discusses the obtained results. Finally, Section 8 concludes the work.

2. Steam generator Degradation and maintenance

The SG is one of the most critical components of a NPP. Its main function is to transfer the heat generated from the reactor core to the secondary fluid (Prusek et al., 2013; Yang et al., 2017; Ayodeji and Liu, 2019). SGs of Pressurized Water Reactors (PWRs) are usually formed by several U-tubes, kept in position using several Tube Support Plates (TSPs), in which the primary fluid flows. The secondary fluid flows through the TSPs in quatrefoil holes surrounding the tubes (Girard, 2014). The heat is transferred from the primary water to the secondary fluid through the tube, generating the steam that is led to the turbine to produce power.

A SG malfunctioning can cause major problems to the whole NPP, with consequences that may lead to serious outages and radioactive releases (Ayodeji and Liu, 2019; Song et al., 2019). The two degradation mechanisms most affecting the SG performance are the TSPs clogging and tube fouling (Varrin, 1996; Corredera et al., 2008; Sollier and Bodineau, 2008; Yang et al., 2017). TSP clogging consists in the progressive reduction of the secondary fluid flow area, caused by the unavoidable deposition of particles and dissolved species present in the water on the quatrefoil holes of the TSP. The reduction of the flow area leads to the formation of high velocity zones that enhance tube vibrations, which may induce tube cracking. Tube fouling consists in the deposition of particles and dissolved species on the tubes themselves. The formation of deposits along the SG tubes leads to an increment of the tube thermal resistance and, as consequence, a reduction of the heat transfer. This causes a reduction of the outlet steam pressure and, consequently, of the NPP overall power production.

Two types of maintenance interventions are periodically performed with the objective of reducing or removing the SG deposits which cause TSP clogging and tubes fouling (Riznic, 2017). On one hand, mechanical cleaning, which is based on the use of high-pressure water jets, allows removing local deposits from the surfaces inside the SG and it is typically performed in one or two days (Riznic, 2017). On the other hand, chemical cleaning is based on the injection of a chemical compound into

the SG. Differently from mechanical cleaning, it removes deposits from the entire SG (private communication, Lacroix, 2012; Weiss et al., 2012; Goujon et al., 2017). To obtain optimum cleaning results in SGs, the chemical cleaning processes should be adapted to the NPP specific history, e.g. water chemistry, material concept, blowdown system design, and the resulting individual prevailing conditions, e.g. deposit amount, constitution and distribution (Rufus et al., 2001; Riznic, 2017). It is a long and expensive maintenance operation, which causes the unavailability of the SG for several hours, can damage some of the SG parts (Prusek, 2012; Girard, 2014) and produces large volumes of chemical wastes. Given the high criticality of SGs and the huge cost associated to their chemical cleaning, the adoption of condition-based maintenance policies based on the estimation of the SG degradation level is crucial (Di Maio, Antonello and Zio, 2018; Hoseyni et al., 2019). To this aim, different types of NDTs, such as televisual and eddy current inspections (Corredera et al., 2008; Yang et al., 2017; Ayodeji and Liu, 2019), have been developed. Televisual inspection (ETV, "*Examens TéléVisuels*") (private communication, Renaud, 2008) visualizes the deposits using a camera inserted from the top of the SG. Its main limitations are that it can be used only to verify the degradation level of the upper part of the SG, and it is very expensive and resource consuming. On the other side, eddy current inspection, which is based on the use of the principle of electromagnetic induction, is faster to be performed and less resource consuming, but it can be applied only if the blockage levels are lower than 50% due to signal saturation problems. Also, its results are remarkably dependent on the shape, density and composition of the deposit (Corredera et al., 2008; Cheong et al., 2011; Girard, 2014).

Other SG degradation monitoring techniques exploit the information content of the Wide Range Level (WRL) signal (Girard, 2014), which is a measure of the pressure difference between the top and the bottom of the SG downcomer. Clogging causes a reduction of the flow area which induces a reduction in the circulation loop flow rate, and, consequently, a smaller pressure drop in the downcomer, which results in a larger wide range level (private communication, Pineau et al., 2016). WRL measurements performed when the SG is in a stationary or steady-state operational regime have been shown to provide less satisfactory diagnostic performances (Girard, 2014) than those obtained considering the WRL behavior during operational transients (Varrin, 1996; Girard et al., 2013; Girard, 2014). However, unexpected WRL measurement jumps caused by sensor recalibration have been reported to be common and to render this technique not accurate enough for the purpose of SG degradation level identification (Girard, 2014).

Methods based on physical models have also been developed to estimate the degradation level of the SG (private communication, Chip et al., 2009; Prusek, 2012; Girard, 2014). Since they usually require the setting of several model parameters, whose values typically vary during the component life and are often very expensive in terms of computational costs, they are not commonly used in practical real time industrial applications.

3. Problem statement

The objective of the present work is to develop a data-driven methodology for the definition of a degradation indicator, d, which quantifies the degradation level of components operating in industrial plants. The methodology for the definition of the degradation indicator relies on the use of signal measurements collected during plant operation and of the results of NDTs periodically performed to assess component degradation.

The available data includes the evolution of K signals collected during operational transients of the same type from Z similar components of a fleet of plants. We indicate with N_z the number of transients collected from the generic *z-th* component of the fleet, and with $N_{tot} = \sum_{z=1}^{Z} N_z$ the total number of transients collected from the entire fleet. The value of the *k-th* signal measured during the n_z-*th* transient of the *z-th* component at time t is indicated by:

$$y_k^{z,\,n_z}(t)\,,\quad \begin{matrix} k=1,\,\ldots,\,K \\ z=1,\,\ldots,\,Z \\ n_z=1,\,\ldots,\,N_z \\ t=1,\,\ldots,\,T_{z,\,n_z} \end{matrix} \tag{1}$$

where T_{z,n_z} represents the duration of the n_z-th transient of the *z-th* component of the fleet. Also, we indicate with ndt_z the number of NDTs performed on the *z-th* component of the fleet and with $D_z(h), h = 1,\ldots, ndt_z$, the degradation level assessed during the generic *h*-th NDT performed on the *z-th* component. Notice that ndt_z is typically much smaller than the number of operational transients, N_z, experienced by the component during its life, due to economic and technical restrictions on performing NDTs.

Notice that, although the methodology for the definition of the degradation indicator can use the NDT results, the final objective of the work is to identify the level of degradation $d^E_{z_{test}}(n_{z_{test}})$ of a test component using only the signal measurements $y_k^{z_{test},n_{z_{test}}}(t),\ k = 1,\ \ldots,\ K$ collected during an operational transient.

4. Method

The method proposed for the definition of a degradation indicator is based on the following steps:

- extraction of a large set of features from the monitored signals. The objective of this step is to condensate the time evolution of a signal during a generic transient, into lumped quantities independent from the time (Section 4.1);
- evaluation of the goodness of the extracted features as degradation indicator, considering its characteristics of monotonicity, trendability and correlability (Section 4.2);
- choice of the most satisfactory features considering a proper trade-off among the different characteristics (Section 4.3);
- construction of the degradation indicator starting from the selected features (Section 4.4).

4.1. Feature extraction

The development of health indicators from the raw measurements $y_k^{z,\,n_z}(t)$ requires a first phase of feature extraction, which aims at extracting J different features, $x_{j,k}^z(n_z)$, $j = 1,\ldots J$ from the evolution of signal k during the generic transient n_z of component z, $y_k^{z,\,n_z}(t)$.

The following features which can potentially contain information on the component degradation are considered:

a Statistical metrics (e.g., mean, standard deviation, kurtosis, skewness, quantile, which are useful to synthetize the general characteristics of the signals even if they are often not suitable for non-stationary signals;
b Signal transforms in the time-frequency domain (e.g., wavelet energy, max coefficient per wavelet component) since this kind of analysis reveals aspects of data often missed by other signal analysis techniques, such as trends, breakdown points, discontinuities in higher derivative and self-similarity (Burrus et al., 1998; Sharp, 2012);
c ad-hoc features (e.g., coefficients of the interpolating parabola) selected after a rough analysis of the signals of the specific case study.

Notice that the quantity $x_{j,k}^z(n_z)$ is explicitly written as a function of the transient n_z to indicate that it describes the component state at the

time in which the n_z-*th* transient occurs.

4.2. Evaluation of the goodness of the extracted features

According to (Coble and Hines, 2009; Coble, 2010; He et al., 2015; Baraldi et al., 2018), a good degradation indicator is characterized by three major desirable properties:

i. Monotonicity; since components typically do not exhibit a self-healing behavior, degradation can only increase as time passes. Therefore, a good degradation indicator is expected to progressively and monotonically increase or decrease with time.
ii. Trendability; a good degradation indicator is expected to show a similar functional evolution during the lives of similar components of the fleet.
iii. Prognosability; a good degradation indicator is characterized by similar values of the feature at the failure times.

Since run-to-failure trajectories are typically not available for safety critical components, which are maintained and repaired to avoid failures, the prognosability of the features cannot be evaluated, and, therefore, this property is not considered in this work.

On the other hand, differently from (Coble and Hines, 2009; Baraldi et al., 2018), we can exploit the information content of the NDTs for the definition of the degradation indicator. To this aim, we introduce the property of:

iv Correlability: if NDTs are performed during the life of the component to assess its degradation level, a good degradation indicator is expected to be correlated with the NDT results.

4.2.1. Monotonicity

The objective is to assess how much the feature $x^z_{j,k}(\cdot)$ shows a monotonic trend. To this aim, two metrics are considered: the first one is based on the Mann-Kendall test (Mann, 1945), whereas the second one is taken from (Coble and Hines, 2009).

The Mann-Kendall test formulates two hypotheses (Gilbert, 1987; Sonali and Nagesh Kumar, 2013; Pohlert, 2015):

- The null hypothesis, H_0, is that the feature values $x^z_{j,k}(\cdot)$, do not have a monotonic trend
- The alternative hypothesis, H_A, is that the feature values $x^z_{j,k}(\cdot)$, have a monotonic trend.

The Mann-Kendall test has been chosen since it does not assume any particular probability distribution of the data, it is not affected by a possible irregular frequency of measurements or by the presence of missing data (Yue and Pilon, 2004). The details of the test are reported in Appendix A.

Considering the *j-th* feature extracted from the *k-th* signal during the life of the *z-th* component along all the transients (from the first $n_Z = 1$ to the last transient $n_Z = N_z$), $x^z_{j,k}(1:N_z)$, the Mann-Kendall test provides a binary outcome, $MK_{j,k,z} = (0,1)$, with 1 indicating that the feature $x^z_{j,k}$ has a monotonic trend and 0 otherwise. The global Mann-Kendall monotonicity index, $M.I^{MK}_{j,k}$, associated to the generic *j-th* feature extracted from the *k-th* signal, $x_{j,k}$, is defined as the average value of the outcome $MK_{j,k,z}$, of the Mann-Kendall test applied to all the Z components:

$$M.I^{MK}_{j,k} = \frac{\sum_{z=1}^{Z} MK(j,k,z)}{Z} \tag{2}$$

Since $MK_{j,k,z}$ can only assume values 0 or 1, a limitation of $M.I^{MK}_{j,k}$ is that it can assume only the discretized values, $0, \frac{1}{Z}, \frac{2}{Z}, \ldots, 1$, which can create a difficulty in the ranking of the features when handling data collected from a small number of similar components, Z.

For this reason, the additional monotonicity index $M.I.^{der}$, based on the study of the feature discrete derivatives proposed in (Coble and Hines, 2009) is also considered. The derivative-based monotonicity index is defined by:

$$M.I^{der}_{j,k,z} = \left| \frac{(\#\Delta > 0) - (\#\Delta \leq 0)}{N_z - 1} \right| \tag{3}$$

$$M.I^{der}_{j,k} = mean_Z\left(M.I_{\cdot,j,k,z}\right) \tag{4}$$

where $\#\Delta > 0$ and $\#\Delta \leq 0$ indicate the number of times the discrete difference $x^z_{j,k}(n_z+1) - x^z_{j,k}(n_z)$ with $n_z = 1, \ldots, N_z - 1$ is positive and negative, respectively, and the denominator in Eq.(3) counts the number of times the discrete difference is computed. Differently from the Mann-Kendall monotonicity index, $M.I^{MK}_{j,k}$, the $M.I^{der}_{j,k}$ derivative-based monotonicity index provides less discretized values within the range [0, 1], being typically $N_z - 1 \gg 0$. Also, in this case, $M.I^{der}_{j,k} = 0$ indicates a completely non-monotonic behaviour, whereas the value of 1 indicates an ideal or completely monotonic behaviour. A limitation of the index, already noticed in (Coble, 2010), is that it is not fully robust with respect to signal noise.

4.2.2. Trendability

In order to measure the trendability of the *j-th* feature extracted from the *k-th* signal collected from the *z-th* component $x^z_{j,k}(1:N_z)$, the index suggested by Cobles and Hines (2009) is here considered:

$$TR_{j,k,z} = \frac{\#\Delta > 0}{N_z - 1} + \frac{\#\Delta^2 > 0}{N_z - 2} \tag{5}$$

$$T.I_{\cdot,j,k} = 1 - std_Z\left(TR_{j,k,z}\right) \tag{6}$$

where $\#\Delta^2 = x^z_{j,k}(n_z+1) - 2x^z_{j,k}(n_z) + x^z_{j,k}(n_z-1)$, with $n_z = 2, \ldots, N_z - 1$, is the number of second order differences. Notice that $TR_{j,k,z}$ is a relative measure of the number of the evaluated positive first Δ, (second, Δ^2) discrete derivatives with respect to the number of the total evaluations of first (second) discrete derivatives of the *j-th* feature extracted from the *k-th* signal collected from the *z-th* component, while, std_Z represents the standard deviation evaluated with respect to the Z similar components. This metric can assume any value in the range [0, 1], where 0 identifies the absence of trendability for the *j-th* feature and 1 represents a perfectly trendable behavior.

4.2.3. Correlability

The quantification of the correlability index $C.I_{\cdot,j,k}$ between the values of a candidate feature and the degradation measurements assessed by means of NDTs is based on:

- the identification of the operational transients that are temporally closest to the performed NDTs. In practice, the *h-th* NDT performed on the *z-th* component, with $z = 1, \ldots, Z$ and $h = 1, \ldots, ndt_z$, is associated to the operational transient n^h_z which is temporally closest to it among the operational transients experienced by component z.
- The computation of the Spearman correlation coefficient among all the available NDT data, $D_z(h)$, with $h = 1, \ldots, ndt_z$, $z = 1, \ldots Z$, collected in the vector $\boldsymbol{D} = [D_1(1), D_1(2), \ldots, D_1(ndt_1), D_2(1), \ldots, D_Z(ndt_Z)]$ and the corresponding feature values $x^z_{j,k}(n^h_z)$, collected in the vector $\boldsymbol{x}_{j,k} = [x^1_{j,k}(n^1_1), x^1_{j,k}(n^2_1), \ldots, x^1_{j,k}(n^{ndt_1}_1), x^2_{j,k}(n^1_2), \ldots, x^Z_{j,k}(n^{ndt_Z}_Z)]$.

The Spearman correlation coefficient allows assessing whether the relationship between the two variables $D_z(h)$ and $x^z_{j,k}(n^h_z)$ can be described by a monotonic function (Spearman, 1904). The advantages of using it instead of other correlation indices are that: *i*) it is relatively

insensitive to outliers; *ii*) it can be used with small sample sizes and *iii*) it is relatively easy to apply (Gauthier, 2001). In practice, the Spearman correlation coefficient is computed by sorting the data in ascending order, considering the value of the positions in the obtained ranking instead of the real value of the data (Myers and Well, 2003), and computing the covariance among the obtained ranked values:

$$C.I._{\cdot j,k} = \frac{cov\left(rg\left(\boldsymbol{x}_{j,k}\right),\ rg(\boldsymbol{D})\right)}{std\left(rg\left(\boldsymbol{x}_{j,k}\right)\right)\ std(rg(\boldsymbol{D}))} \tag{7}$$

where *cov* is the covariance, *std* is the standard deviation and *rg* is the data ranking. The absolute value of the correlability index provides a score in the range [0, 1]: 0 identifies a feature not correlated to the NDT results, whereas 1 refers to a perfectly correlated feature. Notice that, differently from the other indexes, $C.I._{\cdot j,k}$ is directly computed using the data of all the Z components, without the necessity of computing it for each component, z, and, then, averaging. This is due to the fact that the NDT measurements are expected to provide degradation level assessments that can be compared among different components, i.e. in the same scale for all the fleet.

4.3. Features selection

The definition of degradation indicators requires the identification among all the $J{\cdot}K$ features $x_{j,k}$ of those providing the most satisfactory trade-off among the objectives of monotonocity, trendability and correlability. The vector of objective functions $f = (f_1, f_2, f_3, f_4)$ defined by the four indexes $(M.I._{j,k}^{MK},\ M.I._{j,k}^{der}, T.I._{\cdot j,k}, C.I._{\cdot j,k})$ is considered and the Pareto optimal set of features is identified. A feature x_{j^p,k^p} is said to be Pareto-optimal if it is non-dominated, i.e. if does not exist another feature $x_{j',k'}$ such that $f(x_{j',k'})$ dominates $f(x_{j^p,k^p}) : \forall\, i \in (1,\ 2,\ 3,\ 4)\ ,\ f_i(x_{j',k'}) \geq f_i(x_{j^p,k^p}) \ \wedge\ \exists\, \tilde{i} \in (1,\ 2,\ 3,\ 4)\ s.t.\ f_{\tilde{i}}(x_{j',k'}) > f_{\tilde{i}}(x_{j^p,k^p})$ (Baumgartner et al., 2004) (Fig. 1). A limitation of considering the raw values of the calculated indices is that the Pareto optimal set can include features characterized by optimal scores with respect to one index, but very unsatisfactory scores with respect to other indices, leading to an increase of the number of selected solutions. Furthermore, this definition of optimality assumes that all the objectives are characterized by the same relative importance, which is not always necessarily true. Thus, in order to reduce the number of the candidate optimal features and eliminate those with unsatisfactory trade-off among the different objectives, we identify a subset of the Pareto front by assigning a relative importance to the different objectives. In particular, we associate to each objective function, f_i, a weighted utility function (Branke et al., 2001; Baraldi et al., 2009) defined by:

$$\Omega_i(f) = f_i + \sum_{i=1,\ j\neq i}^{4} a_{ij}{\cdot}f_j\ ,\ i,\ j \in (1,\ 2,\ 3,\ 4) \tag{8}$$

where a_{ij} quantifies the amount of gain in the *j-th* objective required to accept a loss of one unit in the *i-th* objective and a_{ii} is by definition equal to 1 (see Fig. 1). The dominance is, then, evaluated with respect to the vectors of objective functions $\Omega = (\Omega_1,\ \Omega_2,\ \ldots,\ \Omega_F)$ with $F = 4$, instead of the vectors f. Fig. 1 shows an example of comparison between the dominance regions of the same candidate solution (point A) when the raw values of the indices f are used (grey region) and when the modified version of the indices Ω is adopted (grey + pink regions), considering two generic objective functions, f_1, f_2. It can be easily noticed that the modified definition of the indices can be translated in a wider dominance region; in particular, in the (f_1, f_2)-plane, the slopes of the dashed lines enclosing the grey region are modified such that the horizontal line (slope = 0) becomes a line with slope $= -1/a_{12}$ while the vertical line (undefined slope) becomes a line with slope $= -a_{21}$. The definition of Ω requires the setting of $F^2 - F$ trade-offs on the basis of the relative importance that the analyst gives to each objective.

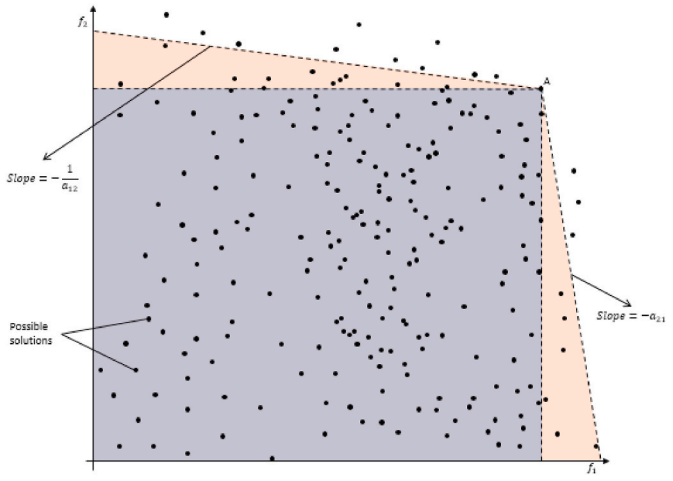

Fig. 1. Schematic representation of the Pareto dominance region of feature 'A' using the raw values of the indices f (grey) and the modified indices Ω (grey + pink). (For interpretation of the references to colour in this figure legend, the reader is referred to the Web version of this article.)

4.4. Construction of the degradation indicator

The objective of this step is to aggregate the features of the Pareto optimal set found in the previous step into a single robust degradation indicator. Since the different features have different units of measurement and ranges, they are firstly normalized on the same scale, which is taken equal to that of the NDTs. In practice, the normalized value, $d_z^{j,k}(n_z)$, of feature j extracted from signal k of component z at time n_z is defined by:

$$d_z^{j,k}(n_Z) = \alpha_{j,k}^z\ x_{j,k}^z(n_Z) + \beta_{j,k}^z \tag{9}$$

where the parameters $\alpha_{j,k}^z\ ,\ \beta_{j,k}^z$ of the linear relationship are independently set for each feature j extracted from signal k of component z using the Ordinary Least Squares (OLS) method with the objective of minimizing the error between the normalized feature value $d_z^{j,k}(n_z^h)$ and the NDT results $D_z(h)$, where n_z^h is the operational transient time closest to the time of the h-th NDT. The estimation of the parameters $\alpha_{j,k}^z, \beta_{j,k}^z$ is complicated by the fact that the NDT results $D_z(h)$ are affected by a measurement error with respect to the unknown ground-truth component degradation. Therefore, the reliable estimation of their values requires the availability of at least two well separated NDT results among those obtained before the n_z-th transient. Specifically, $\alpha_{j,k}^z, \beta_{j,k}^z$ can be estimated only if at least two different NDT results, $D_z(a)$ and $D_z(b), a, b \in [1, \ldots, ndt_z], a \neq b\ D_z(a)$ and $D_z(b), a, b \in [1, \ldots, ndt_z], a \neq b$, which satisfy:

$$|D_z(a) - D_z(b)| > \varepsilon \tag{10}$$

are available, where ε is a preset parameter. The setting of ε should consider the fact that a too small value leads to an unreliable estimation of the parameters $\alpha_{j,k}^z$ and $\beta_{j,k}^z$, since the variation of the NDT results can be the consequence of measurement noise and not of the component degradation, whereas a too large value leads to a delay in the degradation assessment, since several NDTs should be obtained before the condition in Eq. (10) is met and the parameters can be estimated.

Once the features have been normalized, a degradation indicator that estimates the degradation of component z at the occurrence time of transient n_z $d_z^E(n_z)$, is defined by aggregating their values considering their median:

$$d_z^E(n_z) = median_{\{j,\ k\ \in optimal\ pareto\ set\}}\ d_z^{j,k}(n_Z) \tag{11}$$

The median operator has been chosen since it has been shown to be more robust to possible outliers than other operators such as the mean.

5. Procedure for the validation of the degradation indicator

The validation of the proposed methodology requires the use of the results of some NDTs, for the evaluation of the degradation indicator accuracy. A 10-folds cross-validation procedure has been adopted to avoid using the same NDTs data for both the development ("training") of the degradation indicator and the assessment ("testing") of its performance. The components, and consequently their associated data, are randomly divided into 10 folds, then, in an iterative scheme, 9 folds are randomly selected -without repetition- and used for the definition of the degradation indicator (Sections 4.1, 4.2, 4.3 and 4.4), while the remaining fold is used for estimating its accuracy. As accuracy metric, we consider the absolute error between the degradation estimation, $d_z^E(h)$, obtained from the median of the features belonging to the Pareto optimal set and the corresponding NDT measurement $D_z(h)$:

$$e_z(h) = \left|D_z(h) - d_z^E\left(n_z^h\right)\right| \tag{12}$$

Notice that the parameters $\alpha_{j,k}^z$ and $\beta_{j,k}^z$ of the model developed for the estimation of the component degradation level $d_z^E(n_z)$ can be updated each time a new NDT result becomes available. The first error, $e_z(h)$, refers to the third NDT, i.e. $h = 3$, and is based on the estimation of the parameters $\alpha_{j,k}^z$ and $\beta_{j,k}^z$ obtained using the results of the first two NDTs, i.e. $[D_z(1), D_z(2)]$, for each feature belonging to the Pareto optimal set. Once the third NDT has been performed, parameters $\alpha_{j,k}^z$ and $\beta_{j,k}^z$ are newly estimated using the NDT results including the third NDT, $[D_z(1), D_z(2), D_z(3)]$. In this way, the error on the estimation of the 4th NDT can be computed as $e_z(4) = \left|D_Z(4) - d_z^E(n_z^4)\right|$.

The mean error (Eq. (13)) and the error standard deviation (Eq. (14)) of the degradation indicator in the estimation of the degradation of the generic *q-th* NDT test are:

$$E_q = \frac{\sum_{z=1}^{Z_q} e_z(q)}{Z_q} \tag{13}$$

$$\sigma_q = \sqrt{\frac{\sum_{z=1}^{Z_q}\left(e_z(q) - E_q\right)^2}{Z_q}} \tag{14}$$

where Z_q indicates the number of test components that have performed at least q NDTs. Then, the total mean estimation error is:

$$\overline{E} = \frac{\sum_q \left(Z_q\, E_q\right)}{\sum_q Z_q} \tag{15}$$

6. Application to nuclear power plants steam generators

We consider two real case studies involving $Z_1 = 81$ SGs of the 900 MW NPP fleet and $Z_2 = 76$ SGs of the 1300 MW NPP fleet, respectively. All the considered plants are operated by EDF.

The datasets contain the values of $K = 15$ signals describing the plant and the SGs behavior measured within the period 1991–2017 during periodic tests of type EPRGL-4, which are characterized by a decreasing power ramp.

During each transient, the signals are acquired for a 2 h period at a sampling frequency of 0.5 Hz. Fig. 2 shows the time evolution of a measured signal during various transients. Dataset 1 contains a total number of $N_{tot}^1 = 2694$ operational transients of type EPRGL-4 and the results of 99 NDTs performed on the different SGs of the 900 MW fleet, whereas Dataset 2 contains $N_{tot}^2 = 1901$ operational transients and the results of 76 NDTs performed on the different SGs of the 1300 MW fleet. In both case studies the NDT results, which assess the real SGs degradation levels, are obtained by televisual inspection.

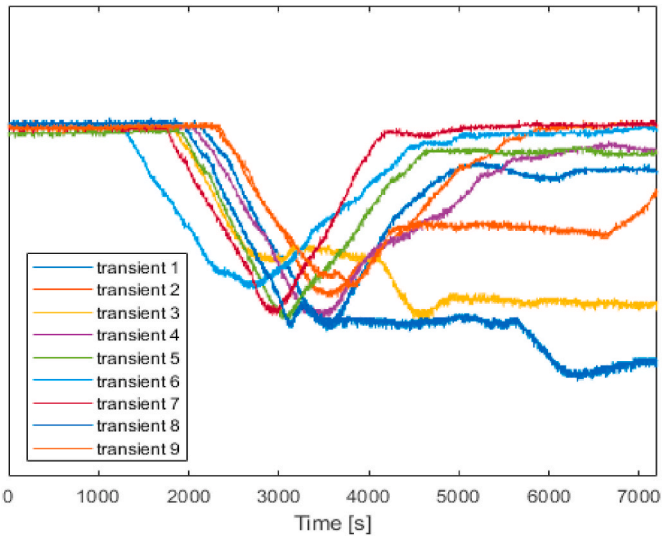

Fig. 2. Time evolutions of a signal during different EPRGL-4 transients in the 900 MW fleet. Measurement values, unit and signal name are omitted for confidentiality.

Although the considered power transients (EPRGL-4) usually last for around 2 h, only the decreasing power ramp is a well standardized and repeatable process, whereas the signal evolution in the remaining part of the transient remarkably depends on the operational conditions and on the demand at the grid side. For this reason, we consider the evolution of the signals during a period of approximately 1200 s, which begins 20 s before the time at which the power starts a decreasing trend and ends 20 s after the time at which it reaches its minimum or 1200 s after the starting point, in the case in which the minimum is not reached. The 20 s interval is added at the beginning and at the end of the period to ensure that the entire transient response to the decreasing ramp is used. The main difference between the two case studies is in the behavior of some signals. For example, the power decrease velocity in case 2 changes over time and the transient duration is relatively shorter (private communication, Vasseur et al., 2016).

7. Results

$J = 93$ features have been extracted from each one of the $K = 15$ signals of interest in both case studies. The threshold ε has been set equal to 0.1, which is an estimation of the degradation assessment error of the televisual inspection NDT.

7.1. 900 MW NPP fleet data

A Pareto optimal set formed by 250 features (out of the extracted 15 × 93) is obtained by assigning the same relative importance to all the objective functions, i.e. considering the raw values of the objective functions, f. Fig. 3-(a) shows the number of Pareto optimal set features extracted from each one of the $K = 15$ monitored signals. Notice that the largest number of features is extracted from signals 10 and 14. Specific information about the considered signals, including their physical nature and units of measurement, cannot be disclosed for confidentiality reasons.

Considering that similar feature trends in different SGs of the same plant can be caused by the fact that they experience the same operational conditions, features with large trendability indexes are not necessarily good degradation indicators. For this reason, we have identified the Pareto optimal set associated to the weighted utility function reported in Table 1, in which the relative importance of the trendability index, $T.I._{j,k}$, is kept lower than the one of the monotonicity

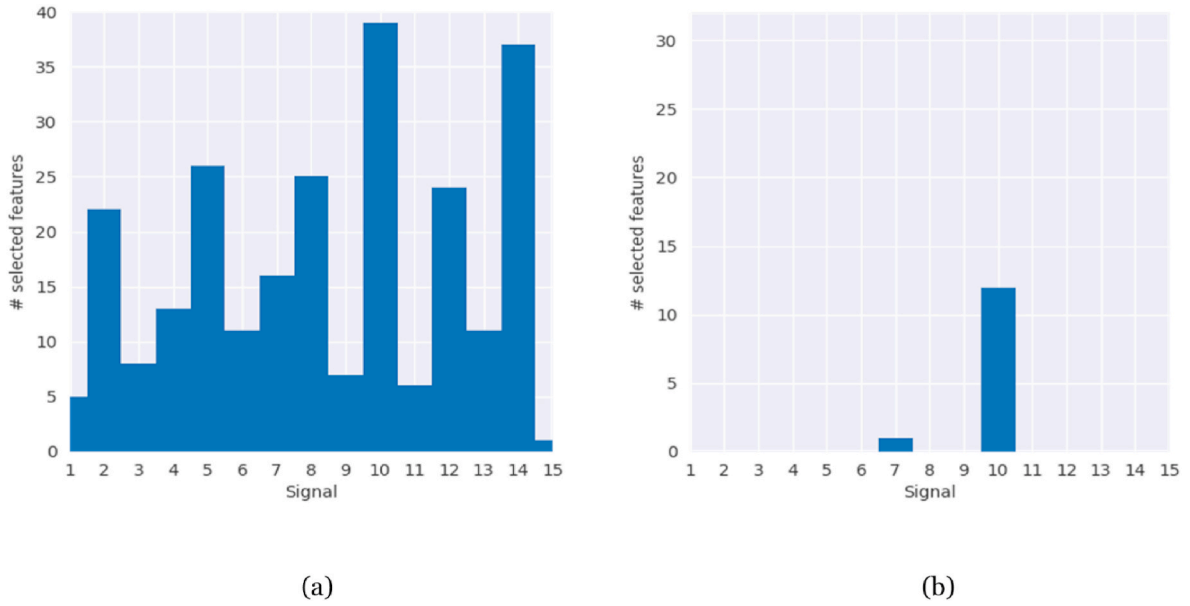

Fig. 3. Distribution of the number of features of the Pareto optimal set extracted from each monitored signal assigning the same weights to all the objectives (a) and the weighted utility function of Table 1 (b).

Table 1
Weighted utility function.

$\Omega_i(f)$	f_i			
	$M.I._{j,k}^{MK}$	$M.I._{j,k}^{der}$	$T.I._{j,k}$	$C.I._{j,k}$
$\Omega_{M.I._{j,k}^{MK}}$	1	0.1	0.02	0.08
$\Omega_{M.I._{j,k}^{der}}$	0.12	1	0.02	0.08
$\Omega_{T.I._{j,k}}$	0.12	0.1	1	0.08
$\Omega_{C.I._{j,k}}$	0.1	0.08	0.02	1

($M.I._{j,k}^{MK}$, $M.I._{j,k}^{der}$) and correlability ($C.I._{j,k}$) indices. Furthermore, considering that noisy features, which are not satisfactory degradation indicators, can have large values of correlability ($C.I._{j,k}$), the relative importance assigned to the monotonicity indices is larger than that assigned to the correlability index. Finally, among the two monotonicity indices ($M.I._{j,k}^{MK}$, $M.I._{j,k}^{der}$), higher importance has been given to $M.I._{j,k}^{MK}$ since it is based on a statistic test.

The Pareto optimal set obtained in this case is formed by 13 features extracted from signals 7 and 10 (Fig. 3-(b)). The results have been verified to be robust with respect to small perturbations in the range ± 0.05 of the entries of the weighted utility function of Table 1.

Notice that the use of the modified objective functions Ω allows significantly reducing the total number of the Pareto optimal set features.

Fig. 4 shows an example of the degradation level estimation obtained using the degradation indicator. In this case, 4 calibration NDT points are needed to calibrate the first linear model (Fig. 4-(a)), since the difference between the first three NDT points is always lower than the threshold $\varepsilon = 0.1$. Notice that when a new NDT is performed (green crosses) the coefficients $\alpha_{j,k}^{q}$ and $\beta_{j,k}^{q}$ of the linear model in Eq.(9) are newly estimated and new, updated estimations of the component degradation levels are obtained (Fig. 4-(b, c)). The degradation level in Fig. 4 is evaluated as percentage of clogging, with 100% indicating the complete occlusion of the quatrefoil holes of the TSP.

Table 2 reports the performance of the degradation indicator obtained using the modified utility function, Ω, in the assessment of the component degradation. The mean error in the estimation of the *q-th* NDT performed on the components, E_q (Eq.(12)), and the total mean estimation error, $\overline{E}$ (Eq.(14)), are considered as error metrics. It can be noticed that the majority of the errors (E_q), is smaller than 10%, which is comparable with the error of the televisual inspection, especially when the degradation level is small.

7.2. 1300 MW NPP fleet data

A Pareto optimal set formed by 103 features is obtained by considering the raw values of the objective functions, f, whereas a Pareto optimal set composed of eight features extracted from signals 10 and 11 is obtained when considering the weighted utility function, Ω, reported in Table 1. Table 3 reports the performance of the degradation indicator developed considering the weighted utility function in the assessment of the component degradation. Also in this case, the majority of the average estimation error, E_q, of the defined degradation indicator is smaller than 10%. Fig. 5 shows an example of degradation level estimation for one SG of the 1300 MW NPP. The obtained results confirm the robustness of the developed method, which is able to give an accurate estimation of the degradation level of different components in different plants operated under different conditions.

8. Conclusions

The adoption of CBM in the nuclear industry requires estimating the degradation level of the plant components. In this work, a novel method for the definition of a degradation indicator for nuclear power plant components is proposed. It allows using two different sources of information: 1) the large amounts of monitored signals collected by the plant supervision system and 2) the few available results of NDTs performed to directly assess the component degradation. The integration of these two sources of information, which is the main methodological contribution of the work, has required the definition of a novel criterion for assessing the goodness of a feature as degradation indicator, and the framing of the feature selection problem as a multi-objective optimization problem.

The proposed method has been applied to the assessment of the degradation level of NPPs SGs, which is currently done by performing very expensive and resource consuming NDTs. The results obtained on real data show its capability of estimating the component degradation level using monitored signals with an error comparable to that of NDTs.

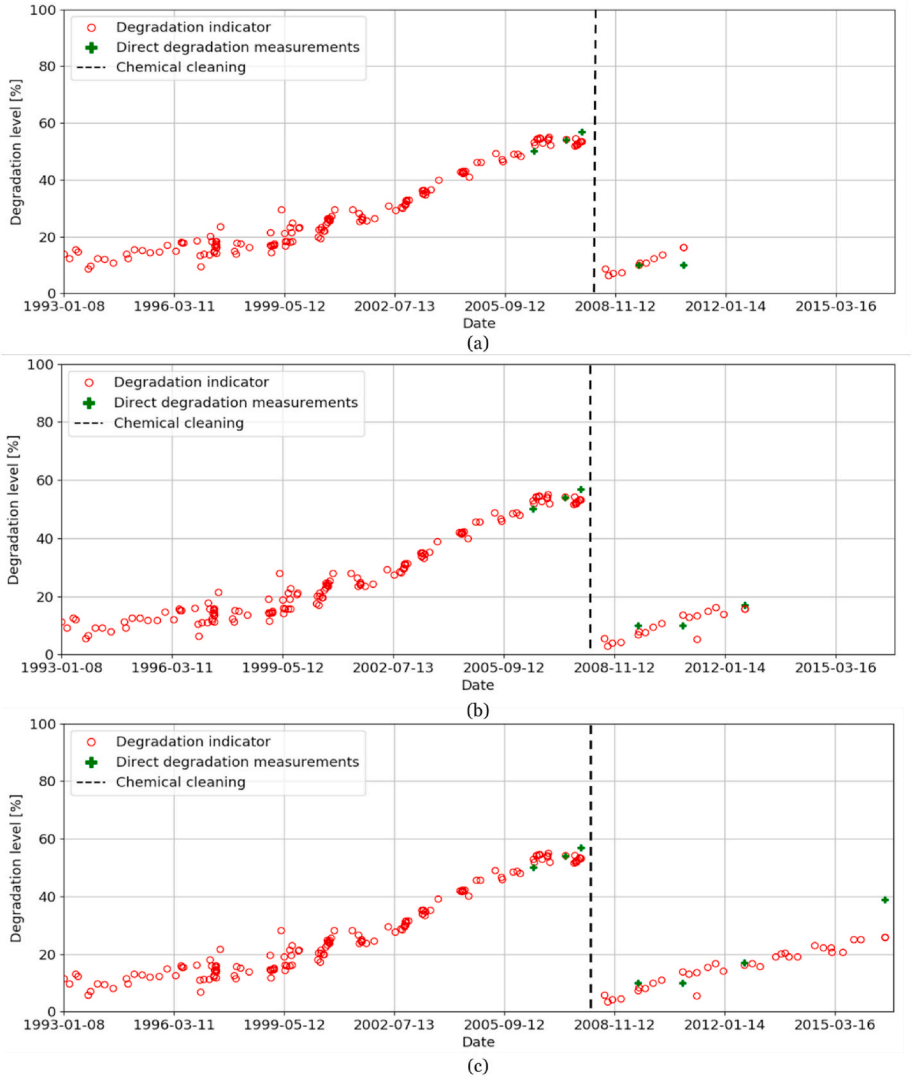

Fig. 4. Estimation of SG degradation level in correspondence of different NDTs performed during its operation.

Table 2
Performance on the 900MW fleet data.

Minimum no. of available q measurements for a unit	No. of units with minimum q available measurements (Z_q)		
3	**7**	E_3	11.5
		σ_3	7.1
4	**6**	E_4	3.2
		σ_4	1.7
5	**5**	E_5	3.3
		σ_5	1.9
6	**5**	E_6	4.9
		σ_6	4.1
7	**2**	E_7	10.7
		σ_7	2.3
Total mean error ($\overline{E}$)			6.2
Total standard deviation			5.4

Table 3
Performance on the 1300 MW fleet data.

Minimum no. of available q measurements for a unit	No. of units with minimum q available measurements (Z_q)		
3	**3**	E_3	9.9
		σ_3	7.9
4	**2**	E_4	1.7
		σ_4	1.3
5	**1**	E_5	12.5
		σ_5	-
Total mean error ($\overline{E}$)			7.7
Total standard deviation			7.0

Credit author statement

Luca Pinciroli, Conceptualization, Methodology, Software, Validation, Formal analysis, Investigation, Writing – original draft, Writing – review & editing, Visualization.**Piero Baraldi**, Conceptualization, Methodology, Formal analysis, Writing – original draft, Writing – review & editing, Supervision. **Ahmed Shokry**, Validation, Formal analysis, Writing – original draft, Writing – review & editing. **Enrico Zio**, Conceptualization, Writing – original draft, Writing – review & editing Supervision. **Redouane Seraoui**, Methodology, Validation, Resources, Data curation, Supervision. **Carole Mai**, Methodology, Software, Validation, Investigation, Resources, Data curation.

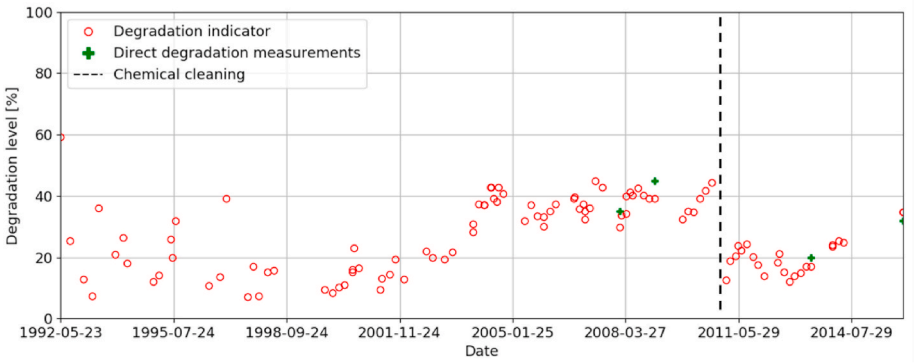

Fig. 5. Degradation level estimation for a SG of a 1300 MW NPP.

Declaration of competing interest

The authors declare that they have no known competing financial interests or personal relationships that could have appeared to influence the work reported in this paper.

Appendix B. Supplementary data

Supplementary data to this article can be found online at https://doi.org/10.1016/j.pnucene.2020.103580.

Appendix A

The Mann-Kendall test statistic characterizing the *j-th* feature extracted from the *k-th* signal collected from the *z-th* component, $S_{j,k,z}$, is calculated according to:

$$S_{j,k,z} = \sum_{n_z^a=1}^{N_z-1} \sum_{n_z^b=n_z^a+1}^{N_z} sgn\left(x_{j,k}^z\left(n_z^a\right) - x_{j,k}^z\left(n_z^b\right)\right) \tag{16}$$

where n_z^a and n_z^b identify any two transients among the N_z available for the *z-th* component and the $sgn(x)$ function is:

$$sgn(x) = \begin{cases} 1 \; if \; x > 0 \\ 0 \; if \; x = 0 \\ -1 \; if \; x < 0 \end{cases} \tag{17}$$

According to (Gilbert, 1987; Sonali and Nagesh Kumar, 2013; Pohlert, 2015), the mean of $S_{j,k,z}$ is zero, i.e. $E[S_{j,k,z}] = 0$ and the variance, $\sigma_{j,k,z}^2$, is given by:

$$\sigma_{j,k,z}^2 = \frac{N_z\,(N_z-1)(2N_z+5) - \sum_{p=1}^{q} t_p\,(t_p-1)\,(2t_p+5)}{18} \tag{18}$$

where t_p is the number of ties for the *p-th* value and q is the number of tied values. By applying the z-transformation (Eq.(19)), a normal distributed variable is obtained.

$$\zeta_{j,k,z} = \begin{cases} \dfrac{S_{j,k,z}-1}{\sigma_{j,k,z}} \; if \; S_{j,k,z} > 0 \\ 0 \; if \; S_{j,k,z} = 0 \\ \dfrac{S_{j,k,z}+1}{\sigma_{j,k,z}} \; if \; S_{j,k,z} < 0 \end{cases} \tag{19}$$

For every component under consideration, this statistic test gives an output, $MK_{j,k,z}$, of value 1 if the null hypothesis is rejected at the α significance level, i.e. data follow a monotonic trend, or 0 if there is insufficient evidence to reject the null hypothesis.

References

Abou-Dakka, M., Bulinski, A., Bamji, S.S., 2011. On-site diagnostic technique for smart maintenance of power cables. IEEE Power and Energy Society General Meeting, IEEE, pp. 1–5. https://doi.org/10.1109/PES.2011.6039394.

Ansean, D., et al., 2017. Lithium-ion battery degradation indicators via incremental capacity analysis. In: *2017* IEEE International Conference on Environment and Electrical Engineering and 2017 IEEE Industrial and Commercial Power Systems Europe. EEEIC/I&CPS Europe), pp. 1–6. https://doi.org/10.1109/EEEIC.2017.7977776.

Ayo-Imoru, R.M., Cilliers, A.C., 2018. A survey of the state of condition-based maintenance (CBM) in the nuclear power industry. Elsevier Ltd Ann. Nucl. Energy 112, 177–188. https://doi.org/10.1016/j.anucene.2017.10.010.

Ayodeji, A., Liu, Y. kuo, 2019. PWR heat exchanger tube defects: trends, signatures and diagnostic techniques. Prog. Nucl. Energy. https://doi.org/10.1016/j.pnucene.2018.12.017.

Baraldi, P., Pedroni, N., Zio, E., 2009. Optimal Power System Generation Scheduling by Multi-Objective Genetic Algorithms with Preferences. Reliability Engineering and System Safety. https://doi.org/10.1016/j.ress.2008.04.004.
Baraldi, P., Bonfanti, G., Zio, E., 2018. Differential evolution-based multi-objective optimization for the definition of a health indicator for fault diagnostics and prognostics. Mech. Syst. Signal Process. 102, 382–400.
Baumgartner, U., Magele, C., Renhart, W., 2004. Pareto optimality and particle swarm optimization. IEEE Trans. Magn. 40 (2), 1172–1175.
Ben Ali, J., et al., 2015. Application of empirical mode decomposition and artificial neural network for automatic bearing fault diagnosis based on vibration signals. Elsevier Ltd Appl. Acoust. 89, 16–27. https://doi.org/10.1016/j.apacoust.2014.08.016.
Branke, J., Kaußler, T., Schmeck, H., 2001. Guidance in evolutionary multi-objective optimization. Adv. Eng. Software 32 (6), 499–507. https://doi.org/10.1016/S0965-9978(00)00110-1.
Burrus, C.S., Gopinath, R.A., Guo, H.T., 1998. La Recherche. 'Introduction to Wavelets and Wavelet Transform—A Primer', vol. 67.
Cheong, Y.M., et al., 2011. Eddy current testing at level 2: manual for the syllabi contained in IAEA-TECDOC-628. Rev. 2 'Training Guidelines for Non Destructive Testing Techniques'.
Chip, V., et al., 2009. 'Etude d'estimation du colmatage par traitement des données de process sur un modèle physique de GV', *Tech. Rep. H-P1B-2009-03213, EDF. Private Communication*, Tech. Rep. In: Tech. Rep. H-P1B-2009-03213, EDF.
Coble, J., 2010. Merging Data Sources to Predict Remaining Useful Life – an Automated Method to Identify Prognostic Parameters. PhD diss. University of Tennessee.
Coble, J., Hines, J.W., 2009. Identifying optimal prognostic parameters from data: a genetic algorithms approach. In: Proceedings of the Annual Conference of the Prognostics and Health Management Society, pp. 1–11. Available at: https://www.phmsociety.org/sites/phmsociety.org/files/phm_submission/2009/phmc_09_69.pdf.
Coble, J.B., et al., 2012. Prognostics and Health Management in Nuclear Power Plants: A Review of Technologies and Applications. US Department of Energy. https://doi.org/10.2172/1047416.
Coble, J., et al., 2015. A review of prognostics and health management applications in nuclear power plants. Int. J. Prognostics Health Manag. 6 (SP3), 1–22.
Corredera, G., Alves-Vieira, M., de Bouvier, O., 2008. 'Fouling and TSP blockage of steam generators on EDF Fleet : identified correlations with secondary water chemistry and planned remedies'. In: Water Chemistry of Nuclear Reactor Systems.
Di Maio, F., Antonello, F., Zio, E., 2018. Condition-based probabilistic safety assessment of a spontaneous steam generator tube rupture accident scenario. Nucl. Eng. Des. https://doi.org/10.1016/j.nucengdes.2017.10.020.
Faudon, V., 2018. Nuclear's digital transormation', *nuclear engineering international*. In: 'WNE Special Edition - New Technology: Encouraging Excellence in Nuclear Energy.
Gauthier, T.D., 2001. 'Detecting trends using spearman's rank correlation coefficient'. Environ. Forensics 2 (4), 359–362. https://doi.org/10.1080/713848278.
Gilbert, R.O., 1987. Statistical methods for environmental pollution monitoring. Technometrics 30 (3), 348.
Girard, S., 2014. Physical and Statistical Models for Steam Generator Clogging Diagnosis. Springer International Publishing. https://doi.org/10.1007/978-3-319-09321-5.
Girard, S., et al., 2013. Sensitivity analysis and dimension reduction of a steam generator model for clogging diagnosis, 113. Reliability Engineering & System Safety, pp. 143–153.
Gomes, P.J.P., et al., 2016. A new degradation indicator based on a statistical anomaly approach. IEEE Trans. Reliab. 65 (1), 326–335.
Goujon, C., et al., 2017. Effects of curative and preventive chemical cleaning processes on fouled steam generator tubes in nuclear power plants. Nucl. Eng. Des. https://doi.org/10.1016/j.nucengdes.2017.07.022.
He, W., et al., 2015. Health monitoring of cooling fan bearings based on wavelet filter. Mech. Syst. Signal Process. 64 (65), 149–161.
Hoseyni, S.M., Di Maio, F., Zio, E., 2019. Condition-based Probabilistic Safety Assessment for Maintenance Decision Making Regarding a Nuclear Power Plant Steam Generator Undergoing Multiple Degradation Mechanisms. Reliability Engineering & System Safety. https://doi.org/10.1016/j.ress.2019.106583.
Huffeteau, S., 2016. Applying digital technologies to strengthen safety and improve competitiveness in the nuclear industry. In: International Congress on Advances in Nuclear Power Plants, ICAPP, pp. 342–346.
IAEA, 2008. On-line Monitoring for Improving Performance of Nuclear Power Plants Part 2: Process and Component Condition Monitoring and Diagnostics. Nuclear Energy Series No. NP-T-1.2, IAEA, Vienna.
IEA, 2017. Digitalisation and energy. IEA, Paris. https://doi.org/10.1787/9789264286276-en. https://www.iea.org/reports/digitalisation-and-energy.
Kumar, S., et al., 2012. A health indicator method for degradation detection of electronic products. Microelectron. Reliab. 52 (2), 439–445. https://doi.org/10.1016/j.microrel.2011.09.030. Elsevier Ltd.
Lacroix, R., 2012. 'Générateurs de vapeur REP AP06/09 – colmatage et encrassement du secondaire des GV – stratégie de maintenance. Tech. Rep. D4550. *01-11/3257 ind. 0*, EDF. Private Communication.
Mann, H.B., 1945. Nonparametric tests against trend. Econometrica 13 (3), 245–259.
Myers, J.L., Well, A.D., 2003. Research Design and Statistical Analysis. Lawrence Erlbaum, London. https://doi.org/10.1360/zd-2013-43-6-1064.
Pineau, D., Vasseur, J., Schwartz, A., 2016. Exigences fonctionnelles pour l'intégration dans le SI-GV de la méthode d'estimation du colmatage par NGL dynamique. Tech. Rep. H-P13-2015-05497-FR, EDF. Private Communication.
Pohlert, T., 2015. Non-parametric trend tests and change-point detection. CC BY-ND 4.0. Available online. http://creativecommons.org/licenses/by-nd/4.0/. (Accessed 25 March 2015).
Prusek, T., 2012. Modélisation et simulation numérique du colmatage à l'échelle du sous-canal dans les générateurs de vapeur *(PhD thesis*. PhD thesis, Aix-Marseille Université).
Prusek, T., et al., 2013. Deposit models for tube support plate flow blockage in Steam Generators. In: Nuclear Engineering and Design, vol. 262. Elsevier B.V., pp. 418–428. https://doi.org/10.1016/j.nucengdes.2013.05.017
Qiu, H., et al., 2003. Robust performance degradation assessment methods for enhanced rolling element bearing prognostics. Adv. Eng. Inf. 17 (3–4), 127–140. https://doi.org/10.1016/j.aei.2004.08.001.
Renaud, C., 2008. 'Evaluation de l'efficacité des NCGV 2007-2008 sur la performance des GV'. Tech. Rep. D4550.31-09/2003. EDF. Private Communication.
Riznic, J., 2017. Steam Generators for Nuclear Power Plants. Woodhead Publishing. https://doi.org/10.1016/C2015-0-01340-5.
Rufus, A.L., et al., 2001. Chemistry aspects pertaining to the application of steam generator chemical cleaning formulation based on ethylene diamine tetra acetic acid. Prog. Nucl. Energy. https://doi.org/10.1016/S0149-1970(01)00004-X.
Saeed, H.A., et al., 2020. Novel fault diagnosis scheme utilizing deep learning networks. Elsevier. In: Progress in Nuclear Energy, vol. 118, p. 103066. https://doi.org/10.1016/j.pnucene.2019.103066. April 2019.
Sharp, M., 2012. Prognostic approaches using transient monitoring methods. Available at: http://trace.tennessee.edu/utk_graddiss/1431/.
Shen, Z., et al., 2012. A monotonic degradation assessment index of rolling bearings using fuzzy support vector data description and running time. Sensors 12 (12), 10109–10135. https://doi.org/10.3390/s120810109.
Shin, J.H., Jun, H.B., 2015. On condition based maintenance policy. J. Comput. Design Eng. 2 (2), 119–127. https://doi.org/10.1016/j.jcde.2014.12.006. Elsevier.
Sollier, H., Bodineau, T., 2008. Tube support plate clogging up of French PWR steam generators. In: Eurosafe 2008 Forum (Paris, France).
Sonali, P., Nagesh Kumar, D., 2013. Review of trend detection methods and their application to detect temperature changes in India. J. Hydrol. 476, 212–227. https://doi.org/10.1016/j.jhydrol.2012.10.034. Elsevier B.V.
Song, J.H., et al., 2019. An analysis on the consequences of a severe accident initiated steam generator tube rupture. Nucl. Eng. Des. https://doi.org/10.1016/j.nucengdes.2019.04.001.
Spearman, C., 1904. The proof and measurement of association between two things. Am. J. Psychol. 15 (1), 72–101. https://doi.org/10.1037/h0065390.
Tambouratzis, T., et al., 2019. Applying the computational intelligence paradigm to nuclear power plant operation: a review (1990- 2015). Int. J. Energy Optim. Eng. 9 (1), 1–50. https://doi.org/10.4018/IJEOE.2020010102.
Tsang, A.H.C., 1995. 'Condition-based maintenance: tools and decision making'. J. Qual. Mainten. Eng. 1 (3), 3–17. https://doi.org/10.1108/13552519510096350.
Uchida, S., et al., 2019. Improvement of plant reliability based on combining of prediction and inspection of crack growth due to intergranular stress corrosion cracking. Nucl. Eng. Des. https://doi.org/10.1016/j.nucengdes.2018.10.021.
Varrin, R.J., 1996. Characterization of PWR steam generator deposits. Tech Rep. EPRI-TR-106048 TRN: 96:002996, Electric Power Research Inst. Dominion Engineering, Inc.
Vasseur, J., Schwartz, A., Pineau, D., 2016. 'Validation de la méthode d'estimation du taux de colmatage par NGL Dynamique sur le GV de type 47/22, 51B, 68/19, 55/19'. Tech. Rep. 6125-3115-2016-16295-FR, EDF. Private Communication.
Wang, H., et al., 2019. A Hybrid Fault Diagnosis Methodology with Support Vector Machine and Improved Particle Swarm Optimization for Nuclear Power Plants. *ISA Transactions*. Elsevier Ltd. https://doi.org/10.1016/j.isatra.2019.05.016.
Weiss, S., Draxler, A., Fandrich, J., 2012. Steam generator maintenance measures as part of an integrated management in PWRs. 3rd International Conference on Nuclear Power Plant.
Yang, G., et al., 2017. A review on clogging of recirculating steam generators in Pressurized-Water Reactors. Prog. Nucl. Energy 97 (May), 182–196. https://doi.org/10.1016/j.pnucene.2017.01.010.
Yue, S., Pilon, P., 2004. A comparison of the power of the t test, Mann-Kendall and bootstrap tests for trend detection. Hydrol. Sci. J. 49 (1), 21–38. https://doi.org/10.1623/hysj.49.1.21.53996.